Fall 2009

Development of pharmacophore and comfa study of rigid and flexible sigma 2 receptor ligands

Hemantbhai Patel
New Jersey Institute of Technology

ABSTRACT

DEVELOPMENT OF PHARMACOPHORE AND COMFA STUDY OF RIGID AND FLEXIBLE SIGMA 2 RECEPTOR LIGANDS

by
Hemantbhai Patel

In the present study a pharmacophore and CoMFA model was derived for sigma 2 (σ_2) receptors by using Sybyl 7.2 Software Package. The CoMFA studies used 22 bioactive molecules as a training set and 4 molecules as a test set for the σ_2 receptor ligands. The geometries and electrostatic charges of all molecules were calculated using various levels of calculations. The geometry optimization and electrostatic charges of all 26 molecules were performed by using semiemprical AM1, ab initio HF/6-31G* and density functional B3LYP/6-31G* in Gaussian 98. The pharmacophore model was derived by using Distance Comparisions (DISCOtech) from 4 partially to highly active σ_2 receptor ligands. The Comparative Molecular Field Analysis (CoMFA) was developed for 22 bioactive σ_2 receptor ligands to investigate a three dimensional quantitative structural activity relationship (3D-QSAR) model for σ_2 receptor ligands. Three CoMFA maps were developed to compare the electrostatic and steric properties of each calculation and molecule. The best CoMFA results were obtained by using a training set of 22 molecules ($R^2 = 0.999$) from B3LYP/6-31G*. The "leave-one-out" cross validation method gave ($q^2 = 0.602$) using four optimal components with optimized geometries and atomic charges. This analysis produced a standard error of estimate of 0.028. The CoMFA results derived from the B3LYP/6-31G* method were better than those from AM1.

DEVELOPMENT OF PHARMACOPHORE AND COMFA STUDY OF RIGID AND FLEXIBLE SIGMA 2 RECEPTOR LIGANDS

by
Hemantbhai Patel

A Thesis
Submitted to the Faculty of
New Jersey Institute of Technology
in Partial Fulfillment of the Requirements for the Degree of
Master of Science in Chemistry

Department of Chemistry and Environmental Science

January 2010

APPROVAL PAGE

DEVELOPMENT OF PHARMACOPHORE AND COMFA STUDY OF RIGID AND FLEXIBLE SIGMA 2 RECEPTOR LIGANDS

Hemantbhai Patel

12/03/09

Dr. Tamara M. Gund, Advisor — Date
Professor of Chemistry, NJIT

12/3/09

Dr. Carol A. Venanzi, Committee Member — Date
Distinguished Professor of Chemistry, NJIT

Dec 3 2009

Dr. Joseph W. Bozzelli, Committee Member — Date
Distinguished Professor of Chemistry, NJIT

BIOGRAPHICAL SKETCH

Author: Hemantbhai Patel

Degree: Master of Science

Date: January 2010

Undergraduate and Graduate Education:

- Master of Science in Chemistry,
  New Jersey Institute of Technology, Newark, NJ, 2010

- Master of Science in Organic Chemistry,
  Sardar Patel University, Vallabh Vidhyanagar, Gujarat, India, 2004

- Bachelor of Science in Industrial Polymer Chemistry,
  Sardar Patel University, Vallabh Vidhyanagar, Gujarat, India, 2002

Major: Chemistry

Dedicated to my beloved family and the scientific community

ACKNOWLEDGEMENT

First and foremost I offer my sincerest gratitude to my advisor, Professor Tamara M. Gund for introducing me to the realm of Molecular Modelling and teaching me the techniques of DISCOtech and CoMFA used to develop the pharmacophore model for Sigma 2 receptor. I am greatly influenced by her kind nature.

It is a pleasure to thank Dr. Joseph W. Bozzelli and Dr. Carol A. Venanzi for being members of my thesis committee. Distinguished Professor Joseph W. Bozzelli gave useful guidance in the use of Gaussian 98 program. Distinguished Professor Carol A. Venanzi gave necessarily guidance and valuable suggestion to improve the quality of my research work. I appreciate their kind help and feel very proud to have great committee members.

My special thanks to Laura Wirpsza for her continuous assistance towards the completion of the project. I am indebted for her generosity in giving her time, knowledge and support with this project.

Thanks to the faculty and staff members of the Chemistry and Environmental Science Department, also Van Houten Library's staff and librarian for their help and support. It seems impossible to prepare final layout of thesis without the help of Dr. Ronald Kane, the Dean of Graduate Studies, and Associate Director Clarisa Gonzalez-Lenahan. I am heartily thankful for their support and encouragement and also to the staff members of the Office of Graduate Studies.

Lastly, I offer my regards to my family and friends for their motivation and encouragement, also everyone who has contributed for my graduate research at New Jersey Institute of Technology.

TABLE OF CONTENTS

LIST OF TABLES

LIST OF FIGURES

CHAPTER 1

INTRODUCTION

Sigma (σ) receptors were first postulated by William Martin in the mid 1970s [1]. The σ receptor was originally classified as an opioid receptor subtype; then it was identified with the phencyclidine (PCP) site on the NMDA receptor channel [2]. The discovery of agents eg. di-tolyl-guanidine (DTG; 25) and various non opioids eg. (haloperidol; 27) led to the realization that σ sites and PCP sites are distinct receptors [3]. Nowadays, σ receptors are well established as non-opioid, non-phencyclidine, and haloperidol sensitive receptor family with its own binding profile and a characteristic distribution in the central nervous system (CNS) as well as in endocrine, immune and some peripheral tissues, like kidney, lung, liver and heart [4]. The σ receptors are divided into three subtypes, termed σ_1, σ_2 [5, 6] and σ_3 receptor [7]. The σ_1 receptor has been cloned from tissues of guinea pig, rat, mouse, and man with the molecular weight of ~25 kDa [8-10]. The σ_2 receptor has not been cloned yet. The molecular weight was estimated to be about 18~21.5 kDa [11]. The σ_3 receptor has been shown to modulate tyrosine hydroxylase (TH) and dopamine synthesis in striatum [12].

Sigma ligands (σ_1 and σ_2) could be used in the treatment of cocaine abuse, depression and epileptic disorders [13, 14]. They also have potential as neuroprotective, antiamnesic, antineoplastic and tumor imaging agents [15, 16]. Both σ_1 and σ_2 sites are found in high densities in a wide variety of human tumors, including those of the breast, lung, colon, ovaries and prostate. While σ_2 sites have been also linked to cellular

proliferation processes and expressed in highly proliferating cells. Several studies have revealed that σ_2 receptor have been associated with apoptosis and produce both transient and sustained increases in calcium ions [17].

There are several selective, high affinity σ_1 ligands available. On the other hand, very few σ_2 selective ligands are known; some of them are shown in Figure 1.1 and the activities of all that compounds are shown in Table 1.1. Haloperidol (27) and di-o-tolyl guanidine (25) bind with high affinity to σ_1 as well as to σ_2 receptors. Examples of series of moderate to highly bioactive σ_2 ligands include: azaperol, related BMY-14802 (4-amino-1-arylbutanols) [18], vesamicol analogues [19], trishmocubane [20], (E)-8-benzylidine-5-(3-hydroxyphenyl)-2-methyl morphan-7-ones derivatives (Table 1.2) [21], N-alkylazacycloheptane derivatives [22], 1-cyclohexylpiperazine derivatives (Table 1.3) [23], 1-aralkyl-4-benzylpiperidine (Table 1.4) and 1-aralkyl-4-benzylpiperazine derivatives (Table 1.5) [24], and N-substituted 9-azabicylo [3.3.1] nonan-3α-yl carbamate analogues [25].

Several molecular modelling studies have been performed to define the binding pharmacophore model for different classes of σ ligands. Manallack used various classes of molecules to determine the first σ_1 pharmacophore [26]. Glennon and Gund have also proposed selective σ_1 pharmacophore models [27, 28]. Laggner et al. discovered pharmacophore models built with catalyst software which based upon a series of 23 structurally diverse chemical compounds [29].

A pharmacophore model for the σ_2 receptor was derived by using GRIND (Grid Independent Descriptors), however the program does not require ligand alignment.

PLS models for the σ_2 affinity had r^2=0.83 and q^2=0.63 were derived using a series of α-tropanyl derivatives. This model provides internal geometrical relationships within two hydrophobic areas (hydrophobic-1 and 2) and H-bond donor receptor region with which ligands establish non covalent bonds [30]. The goal of these computational studies was the development of a binding model which could accommodate the array of compounds that have affinity for the σ_2 receptor.

Figure 1.1 Rigid and Flexible σ_2 Receptor Ligands.

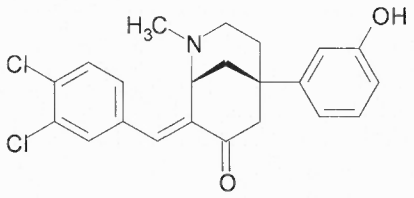

CB-184 (4)

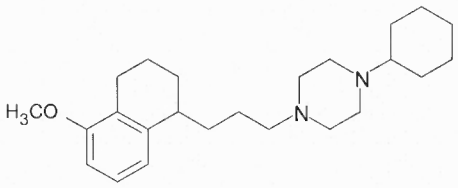

PB-28 (6)

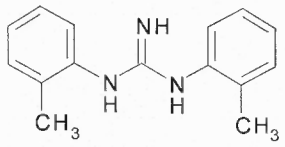

1,3-di-o-tolyl guanidine (DTG) (25)

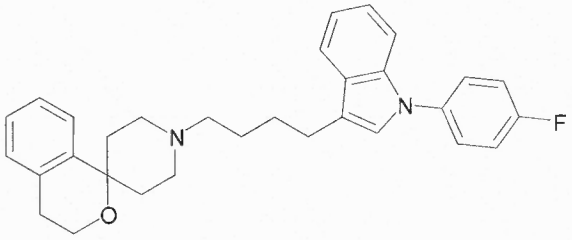

Spiro[(2)benzopyran-1,4'-piperidine] Derivative (26)

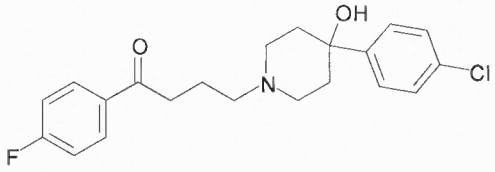

Haloperidol (27)

Table 1.1 Binding and Functional Data of Rigid and Flexible σ_2 Receptor Ligands [21, 23, 24]

Compounds	Configuration	σ_1 K_i(nM)	σ_2 K_i (nM)	σ_1/σ_2
4*	(+)-1R,5R	7436	13.4	554.93
6*	-	13.6	0.34	40.00
25*	-	69	21	3.29
26*	-	41.43	0.7	59.19
27	-	2.2	16	0.14

Note: * Indicates included in Pharmacophore Derivation. † Indicates included in CoMFA test set

Table 1.2 Binding and Functional Data of (E)-8-benzylidene-5-(3-hydroxyphenyl)-2-methylmorphan-7-ones [21]

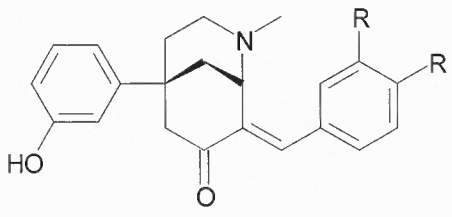

(-)-1S, 5S

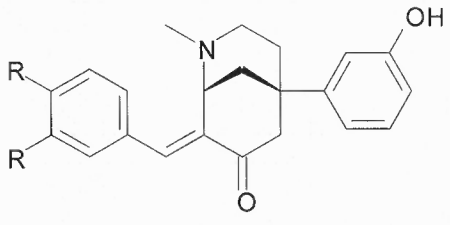

(+)-1R, 5R

(1) CB-64L, R=H
(3) CB-182, R=Cl

(2) CB-64D, R=H
(4) CB-184, R=Cl

Compounds	Configuration	σ_1 K_i(nM)	σ_2 K_i (nM)	σ_1/σ_2
1	(-)-1R,5R	10.5	154	0.07
2†	(+)-1R,5R	3063	16.5	185
3	(-)-1R,5R	27.3	35.5	0.77
4*	(+)-1R,5R	7436	13.4	554

Note: * Indicates included in Pharmacophore Derivation. † Indicates included in CoMFA test set.

Table 1.3 Binding and Functional Data of 1-cyclohexylpiperazine Derivatives [23]

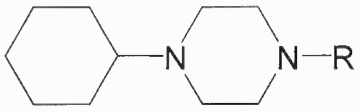

Compounds	R	σ_1 K_i (nM)	σ_2 K_i (nM)	σ_1/σ_2	σ_2/σ_1
5†	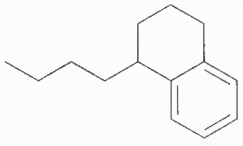	0.61	0.68	0.90	1.11
6*	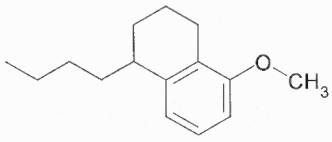	13.6	0.34	40.00	0.03
7	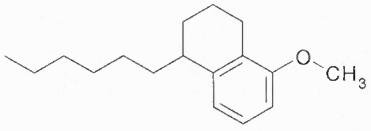	1.52	0.35	4.34	0.23
8	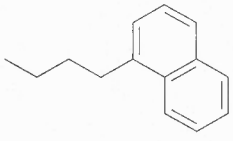	2.16	0.69	3.13	0.32
9	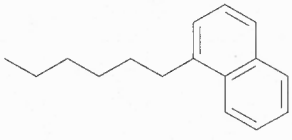	2.4	0.57	4.21	0.24

Note: * Indicates included in Pharmacophore Derivation. † Indicates included in CoMFA test set.

Table 1.4 Binding and Functional Data of 1-aralkyl-4-benzylpiperidine Derivatives [24]

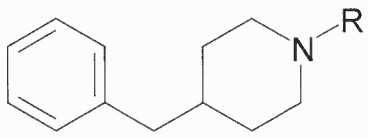

Compounds	R	σ_1 K_i (nM)	σ_2 K_i (nM)	σ_1/σ_2	σ_2/σ_1
10	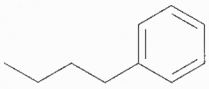	1.40	0.49	2.86	0.35
11†	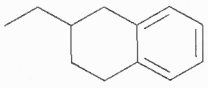	1.50	2.52	0.60	1.68
12	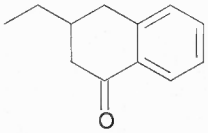	1.40	4.63	0.30	3.31
13	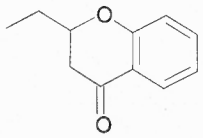	1.40	7.90	0.18	5.64
14	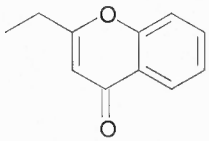	115	285	0.40	2.48

Note: * Indicates included in Pharmacophore Derivation. † Indicates included in CoMFA test set.

Table 1.5 Binding and Functional Data of 1-aralkyl-4-benzylpiperazine Derivatives [24]

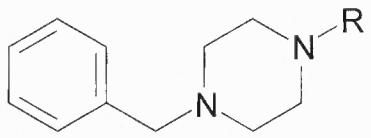

Compounds	R	σ_1 K_i (nM)	σ_2 K_i (nM)	σ_1/σ_2	σ_2/σ_1
15	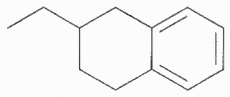	0.80	1.70	0.47	2.13
16	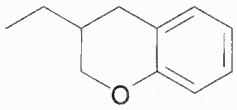	0.30	1.48	0.20	4.93
17	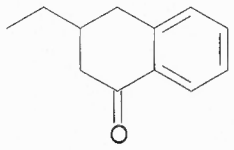	0.30	1.59	0.19	5.30
18	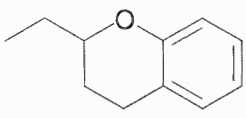	0.30	3.02	0.10	10.07
19†	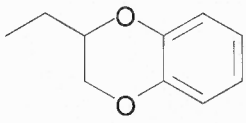	15.4	25.6	0.60	1.66
20	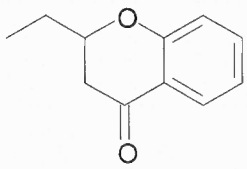	1.20	4.75	0.25	3.96
21	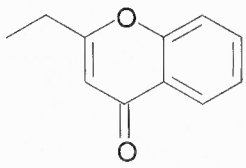	2.66	5.35	0.50	2.01
22	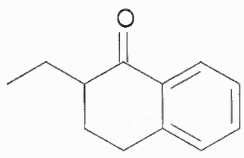	0.40	1.40	0.29	3.5
23	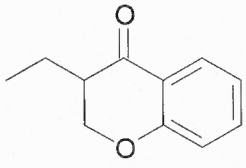	18	32.8	0.55	1.82

24	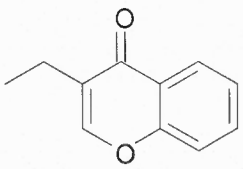	3.80	14.1	0.27	3.71

Note: * Indicates included in Pharmacophore Derivation. † Indicates included in CoMFA test set.

CHAPTER 2

PHARMACOPHORE DERIVATION

2.1 Materials and Methods

The calculation in this study was carried out using SYBYL 7.2 [31] molecular modeling program. All ligands used in this study were built using SYBYL 7.2, and then energy minimized using the Tripos force field. The geometry optimization and atomic charges calculation of all molecules used in this study was performed by AM1, HF/6-31G* and B3LYP/6-31G* methods by using Gaussian 98 program [32]. The pharmacophore was derived from a set of active compounds by DISCOtech using SYBYL 7.2. DISCOtech considers all possible mappings of features starting from a set of representative conformers for each molecule to create a set of alignments. The CoMFA models were derived using SYBYL 7.2. The CoMFA methodology is a 3D quantitative Structure-activity relationship (QSAR) technique which ultimately allows designing and predicting activities of molecules.

2.2 Selection of Ligands

Ligands can interact either covalently or noncovalently with their biological target. The noncovalent, reversible association of receptor (R) and ligand (L) to form a receptor-ligand complex (R'L') generally occurs in an aqueous, electrolyte-containing solution (Equation 2.1).

$$R_{aq.} + L_{aq.} \leftrightarrow R'L'_{aq} \qquad (2.1)$$

Under thermodynamic equilibrium conditions, this reaction is determined by the standard Gibb's free energy of binding ΔG^0. This quantity is related to the experimentally determined association constant K_A (or its reciprocal dissociation or inhibition constants, K_D or K_i, respectively) (Equation 2.2).

$$K_A = K_D^{-1} = K_i^{-1} = [R'L']/[R]\,[L] \tag{2.2}$$

ΔG^0 is composed of an enthalpic (ΔH^0) and an entropic ($T\Delta S^0$) portion. T refers to the absolute temperature. In place of ΔG^0, the term (binding) affinity is used to describe the tendency of a molecule to form a complex with another one (Equation 2.3) [33].

$$\Delta G^0 = -RT\ \ln K_A = \Delta H^0 - T\Delta S^0 \tag{2.3}$$

The compounds for σ_2 pharmacophore derivation were based on potency, selectivity, and structural diversity. The pharmacophore for σ_2 was defined by using four moderate to highly active compounds. Among four compounds selected, there were two rigid ligands: DTG (25) and CB-184 (4) and two flexible ligands: PB-28 (6) and spiro[(2)benzopyran-1,4'-piperedine] derivative (26). These are listed in Table 1.1 with relative binding affinity and selectivity values. The relative σ_2 binding value for all four ligands in Table 1.1 ranges from 0.34 to 13.4 nm. The σ_1/σ_2 ratio of four compounds in Table 1.1 ranges from 3 to 555 indicating high selectivity for the σ_2 receptor. Binding assays were performed using [^{3}H] di-tolyl-guanidine and [^{3}H] (+) pentazocine [11]. The K_i values were converted to pK_i values by using below Equation 2.4.

$$pK_i = -\log [K_i] \quad (2.4)$$

2.3 Choice of Initial Conformations

All structures used in this study were generated by building with SYBYL 7.2 using default bond distances and angles. The energy minimization of all ligands was carried out by using the tools MAXIMIN2. The tripos force field with a distance-dependent dielectric function was applied. The maximum number of iterations was set to 100 with nonbonded (NB) cut off, 8.0 A^0 and convergence criterion of 0.05 Kcal/mol of energy difference between successive iterations.

2.4 Pharmacophore

A pharmacophore is commonly defined as an arrangement of molecular features or fragments forming a necessary but not sufficient condition for biological activity. A three-dimensional (3-D) pharmacophore is defined by a critical geometric arrangement of such features or fragments. Pharmacophores have traditionally been applied singly as inputs for 3-D database searching, molecular graphics, or automated 3-D design and 3D-QSAR (Quantitative Structure-Activity Relationship) methods [34]. DISCO (DIStance Comparison) [35] program; developed by Martin for the purpose of identifying and systematically aligning common pharmacophoric elements among structurally diverse ligands was used to derive a pharmacophore model for σ_2 ligands. DISCOtech identifies all potential pharmacophoric site points in each molecule of the database. The most common properties used to describe the potential pharmacophoric fetures of a structure are:

(i) Hydrogen bond donor, such as primary/secondary amide, aniline nitrogens and hydroxyl.

(ii) Hydrogen bond acceptor, for example carbonyl, aliphatic ether and hydroxyl.

(iii) Basic (positively charged at physiological pH 7), for example sp^3 N aliphatic amines, hydrazines, guanidines and 2/4 amino pyridines.

(iv) Acidic (negatively charged at physiological pH 7), such as carboxylic acid, acyl sulfonamide, unsubstituted tetrazole and phenols.

(v) Aromatic, generally (but not always) in the form of ring centroids.

(vi) Hydrophobic, for example certain 5/6 membered aromatic rings, isopropyl, butyl and cyclopentyl.

The conformer databases were generated for all compounds by DISCOtech. Only unique conformers were included in databases, the rest were effectively excluded by Discotech. A master database containing one low energy conformer of each molecule was utilized as a starting point for the DISCO program [36]. By utilizing DISCO, binding models were found with two hydrophobic regions and a nitrogen center. These all DISCO models were then inspected visually in an effort to eliminate models that may not represent an intuitively rational molecular alignment. The close inspection revealed that the model shown in Figure 2.1 represents the most rational alignment when considering the structural diversity of all 22 compounds in the training set. The pharmacophore triangle includes a nitrogen center and two hydrophobic regions.

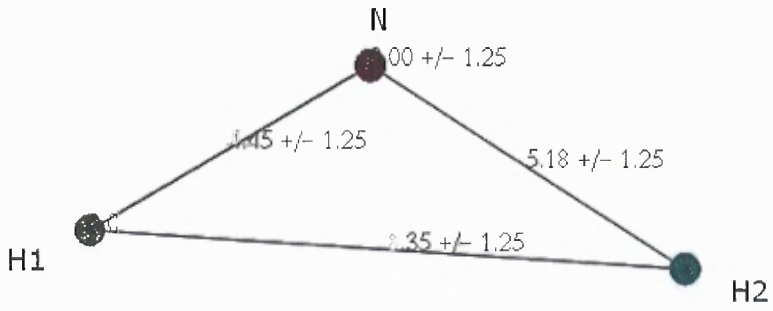

(a)

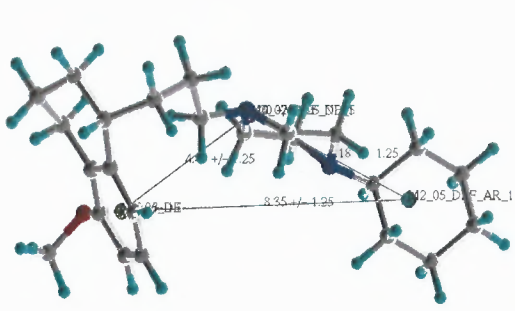

(b)

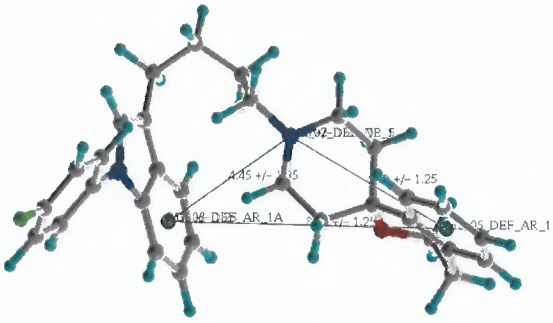

(c)

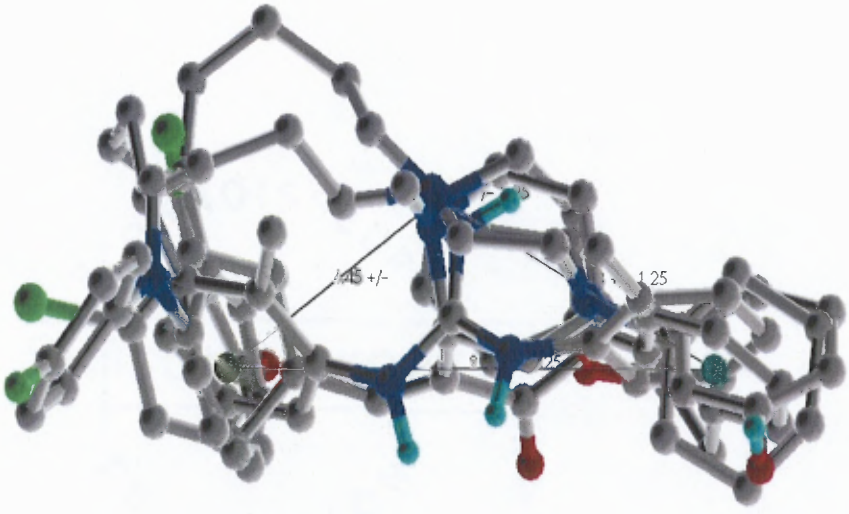

(d)

Figure 2.1 DISCOtech Pharmacophore dimensions with hydrophobic (H1 and H2) regions, nitrogen (N) (a); DISCOtech model with σ_2 receptor ligands 6 (b) and 26 (c) respectively, and also with all four ligands 4, 6, 25 and 26 (d).

CHAPTER 3

CoMFA STUDIES

3.1 Geometry Optimization and Electrostatic Studies

The GAUSSIAN 98 program was used to optimize the conformers derived by DISCOtech. The calculation of electrostatic charges for these geometries were performed using semi empirical AM1, density functional B3LYP/6-31G*, and ab initio HF/6-31G* levels according to Mulliken populations.

3.2 Alignment

An alignment of the training and test set molecules is essential for a CoMFA Studies. The three optimized calculations were aligned by a match function in SYBYL 7.2 using a template molecule (25) in Table 1.1 and with the generated pharmacophore in Figure 2.1. All 26 molecules were aligned with respect to their class and overall geometry by using the ALIGN DATABASE and 'Field Fit' functions in SYBYL 7.2. The aligned 26 molecules of training and test set are represented in Figure 3.1 according to their optimization method [37].

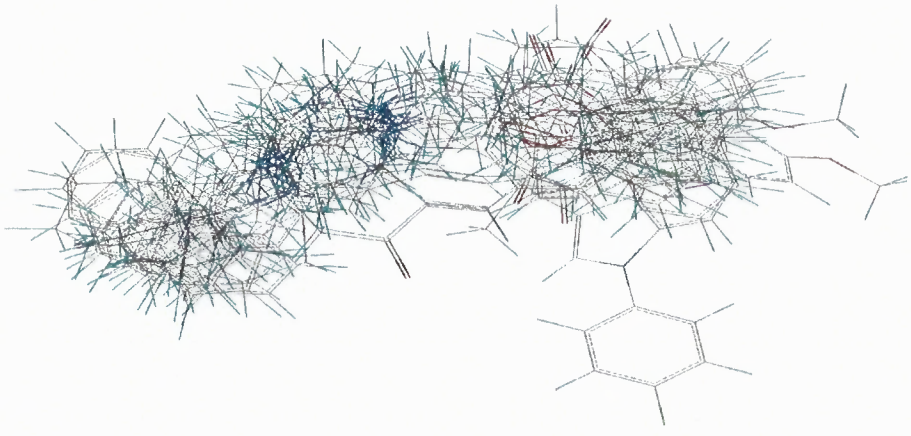

(a)

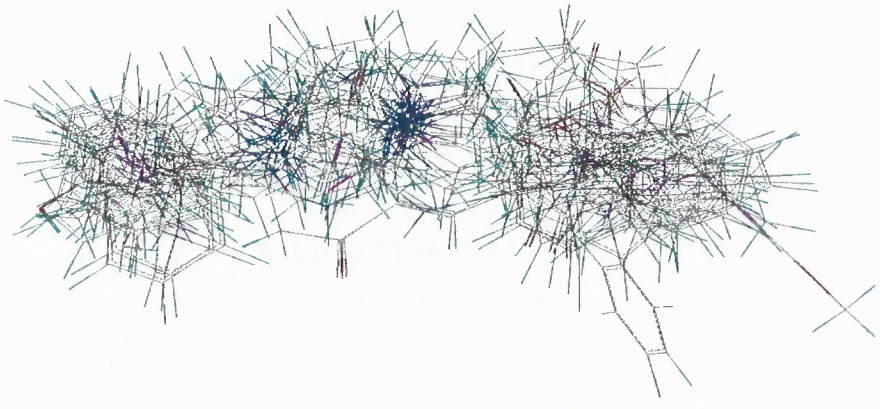

(b)

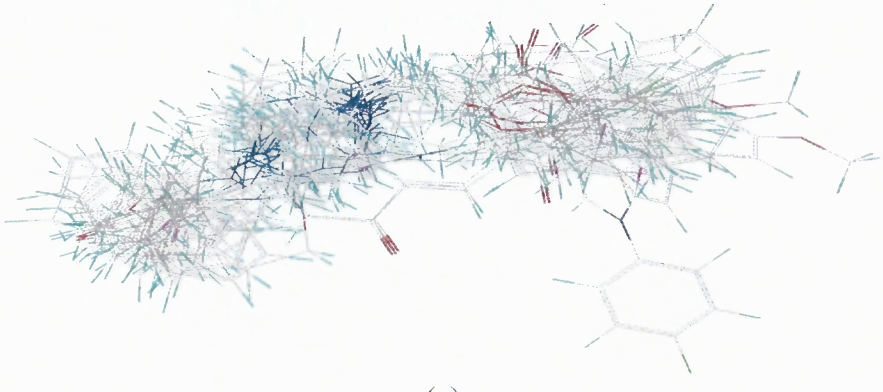

(c)

Figure 3.1 Alignments of all 26 molecules optimized using: AM1 (a), HF/6-31G* (b) and B3LYP/6-31G* (c) methods.

3.3 CoMFA Model

The CoMFA studies were carried out using the QSAR option of SYBYL 7.2. CoMFA methodology is based on the assumption that drug-receptor interactions are non-covalent and change in biological activity correlate with the changes in the steric and/or electrostatic fields of the drug molecules. The three must-obey rules should be followed in three dimentional quantitative structure –activity relationship (3D-QSAR) to achieve a quality CoMFA model: (i) the training set must include a wide population (at least 16 items) of diverse compounds covering at least 4 orders of magnitude of activity; (ii) the most active compound should be included in the training set; (iii) all biological data must be obtained by homogeneous procedures [38, 39].

A comprehensive CoMFA analysis was initiated, once model Figure 2.1 was chosen from the DISCO results as the most appropriate pharmacophore alignment. The process of developing a suitable CoMFA model required the evaluation of various training sets utilizing both cross validated and non-cross validated methods. The auto CoMFA columns were generated using the Tripos Standard CoMFA field class. A sp^3 hybridized carbon atom was probed with the default grid spacing, and a charge of +1.0 with a dielectric function of 1/r; a dielectric constant ε of 1 extends 4.0 Å beyond every molecule in all directions. The default of 30 kcal/mol energy cutoff for steric and electrostatic fields was used [40].

As far as the steric field is concerned, this will increase as the probe atom gets closer to the molecule. As far as the electrostatic field is concerned, there will be an attraction between the positively charged probe and electron-rich regions of the molecule, and repulsion between the probe and electron-deficient regions of the molecule.

A particular value for the steric energy is then chosen which will define the shape of the molecule, and the grid points having that value are then connected by contour lines to define the steric field. This is done for each molecule. A similar process is carried out to measure the electrostatic interactions between the positively charged probe atom and the test molecule. Electron-rich and electron-deficient regions for each molecule are then defined by suitable contour lines. After defining the size, shape and electronic distribution of series of molecules, the next stage is to relate these properties to the biological activity of the molecules.

The SAMPLS (SAMple-distance PLS) algorithm developed by Bush and Nachbar [41] was used to determine q^2 value by "leave-one-out" cross validation. Essentially, it is an analytical computing process which is repeated over and over again (iterated) to try to find the best formula relating biological property against the various variables. Once a formula has been defined, the formula is tested against the structure which was left out. This is called cross-validation and tests how well the formula predicts the biological property for the molecule which was left out. The results of this are fed back into another round of calculations, but now the structure which was left out is included in the calculations and a different structure is left out. This leads to a new improved formula which is once again tested against the compound that was left out, and so the process continues until cross-validation has been carried out against all the structures. At the end of the process, the final formula is obtained. For each molecule n, this QSAR is results in the Equation 3.1.

$$\text{Affinity}_n = k + \alpha_1 S_{n,1} + \ldots + \alpha_M S_{n,M} + \beta_1 E_{n,1} + \ldots + \beta_M E_{n,M} \qquad (3.1)$$

The indices 1, 2, ..., M reflect the respective grid points, and $S_{n,1}$,..., $S_{n,M}$ and $E_{n,1}$, ..., $E_{n,M}$ describe steric and electrostatic energies at these points. The coefficients α_1, ..., α_M and β_1, ..., β_M are obtained from a system of linear equations by partial least-squares analysis [42]. The predictability of this final equation is quantified by the cross-validated correlation coefficient r^2, which is usually referred to as q^2 PRESS (predictive residual sum of squares).

The bioactivities of CB-64L (1) and CB-182 (3) were poor as σ_2 ligands and the exclusion of both of these compounds from CoMFA model showed a decreased cross-validated $r^2 = 0.357$ with two components and $q^2 = 0.315$ by "Leave-one-out" cross-validation for set of molecules optimized by HF/6-31G* method. Addition of one more compound (14); the most inactive σ_2 ligand to CoMFA training set of HF/6-31G* optimized molecules showed an increased cross-validated $r^2 = 0.446$ with three components and $q^2 = 0.496$ at three components by the "Leave-one-out" cross-validation method so this CoMFA study was done on 3 orders of Log difference between the most active and most inactive ligand included in the training set. The best CoMFA results obtained from these analyses are listed in Table 3.1. The threshold q^2 value of 0.5 is considered to be minimal for a significantly internally predictive model [43]. The cross-validation method was utilized to find out predictive power of CoMFA model and to decide how many components to use for the best model. The 5% rule was considered to determine this number of optimal components, if q^2 increases by at least 5% upon increasing the number of components by one, then it is justified to add an additional component [44]. The Experimental and Predicted bioactivity for all 22 compounds of Training set are listed in Table 3.2 and for the test set compounds are listed in Table 3.3.

A Graph of actual activities versus predicted activities of the all compounds are shown in Figure 3.2.

Table 3.1 Optimal Component Number and q^2 by "Leave-One-Out" by SAMPLS [38] using the Training Set of 22 Molecules

Theory	Terminology	Comp. 1	Comp. 2	Comp. 3	Comp. 4
AM1	standard error	0.753	0.685	**0.687**	0.714
	q2 (PRESS)	0.222	0.387	**0.417**	0.404
HF/6-31G*	standard error	0.737	0.653	**0.646**	0.667
	q2 (PRESS)	0.254	0.443	**0.484**	0.480
B3LYP/6-31G*	standard error	0.678	0.600	0.517	**0.584**
	q2 (PRESS)	0.368	0.529	0.597	**0.602**

Table 3.2 Experimental and Predicted Bioactivities (pK_i) for the Training Set of 22 Molecules using Various Calculation Methods

Compounds	Lit. pK_i	AM1	HF/6-31G*	B3LYP/6-31G*
			Predicted pK_i	
1	-2.188	-2.096	-2.084	-2.156
3	-1.550	-1.597	-1.594	-1.583
4	-1.127	-1.140	-1.148	-1.143
6	0.469	0.476	0.454	0.466
7	0.456	0.378	0.446	0.457
8	0.161	0.162	0.197	0.155
9	0.244	0.233	0.235	0.256
10	0.310	0.258	0.361	0.278
12	-0.666	-0.655	-0.709	-0.643
13	-0.898	-0.900	-0.940	-0.883
14	-2.455	-2.537	-2.454	-2.469
15	-0.230	-0.316	-0.259	-0.234
16	-0.170	-0.161	-0.176	-0.141
17	-0.201	-0.218	-0.113	-0.184
18	-0.480	-0.382	-0.430	-0.458
20	-0.677	-0.687	-0.617	-0.633
21	-0.728	-0.825	-0.700	-0.745
22	-0.146	-0.107	-0.140	-0.148
23	-1.516	-1.415	-1.490	-1.531
24	-1.149	-1.246	-1.222	-1.190
25	-1.322	-1.269	-1.368	-1.288
26	0.155	0.229	0.159	0.112

Table 3.3 Experimental and Predicted Binding Affinities (pK_i) for Test Set of Four Molecules using Various Calculation Methods

Compounds	Lit. pK_i	AM1	HF/6-31G*	B3LYP/6-31G*
2	-1.217	-1.325	-1.262	-1.322
5	0.167	0.226	0.105	0.324
11	-0.401	-0.437	-0.463	-0.587
19	-1.408	-1.218	-1.358	-1.448

The final CoMFA analysis were carried out with CoMFA standard scaling, crossvalidated q^2, conventional (non-cross validated) r^2, F statistic, Standard error of estimate, Steric and Electrostatic field co-efficient and fraction of contribution values were calculated and are presented in Table 3.4. This analysis generated predictive models and CoMFA co-efficient contour diagrams for the steric and electrostatic potential contributions are displayed in Figure 3.3. The CoMFA contour maps of steric fields are shown in yellow and green. The steric regions define the size and shape of the substituents around the molecule. The green areas (80% contribution) are areas where more bulky substituents are favoured, and yellow (20% contribution) are areas where less bulk is desired for higher σ_2 activity. The contour maps of electrostatic fields are shown in red and blue color. The red areas (80% contribution) are regions that favor more negative charge, and blue areas (20% contribution) are areas that favor more positive charge for higher σ_2 activity.

Table 3.4 QSAR Reports by Non-Crossvalidation using SAMPLS [38] by the Training Set of 22 Molecules

Theory	S.E.	R^2	F Values	Steric.	Electro.
AM1	0.080	0.992	(n1=4, n2=21) 623.700	0.303	0.697
HF/3-21G*	0.052	0.996	(n1=4, n2=21) 1493.392	0.358	0.642
B3LYP/3-21G*	0.028	0.999	(n1=4, n2=21) 4610.975	0.301	0.699

Note: Standard error of estimation, R^2 of non-crossvalidation using training set of 22 molecules in Table 1.2-1.5. Steric and Electrostatic contributions to this CoMFA field.

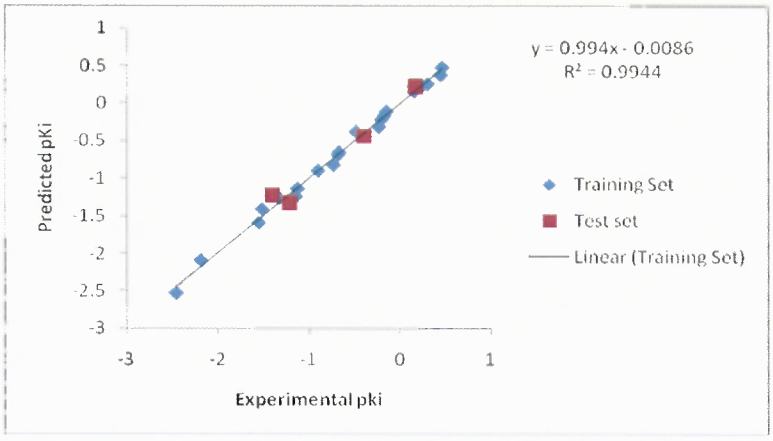

(a)

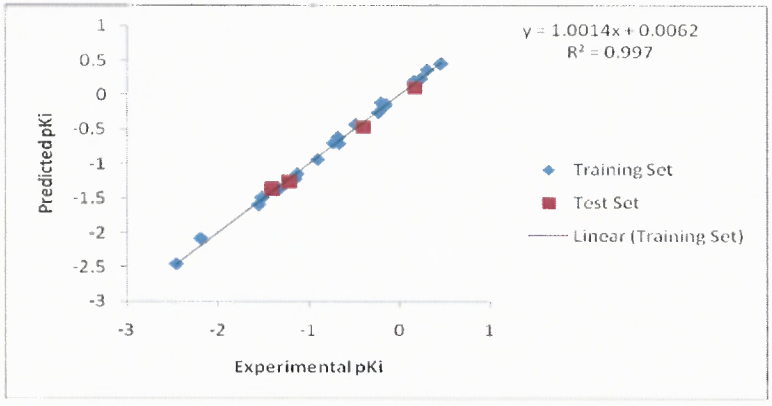

(b)

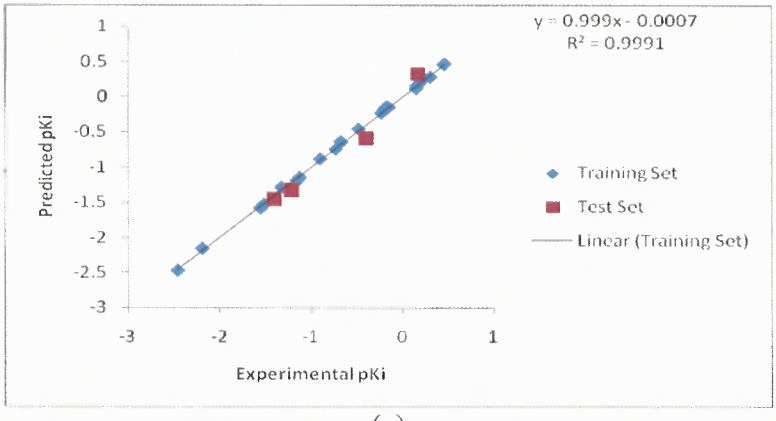

(c)

Figure 3.2 Graph of experimental (pK_i = -log [K_i]) versus predicted bioactivity by the CoMFA model using different calculation methods AM1 (a) HF/6-31G* (b) and B3LYP/6-31G* (c).

Note: *Blue indicates training set while red indicates test set.

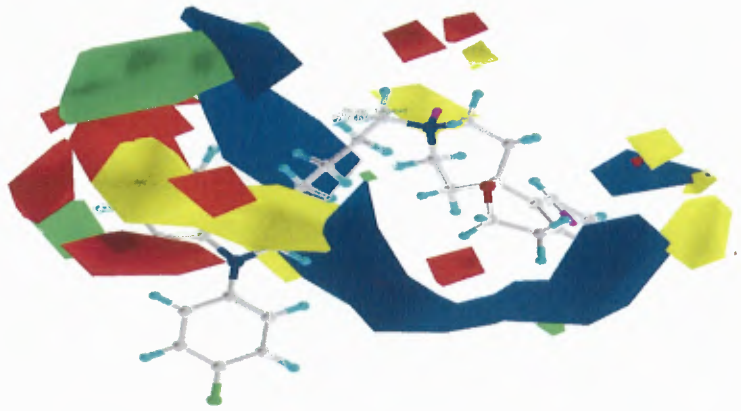

(a)

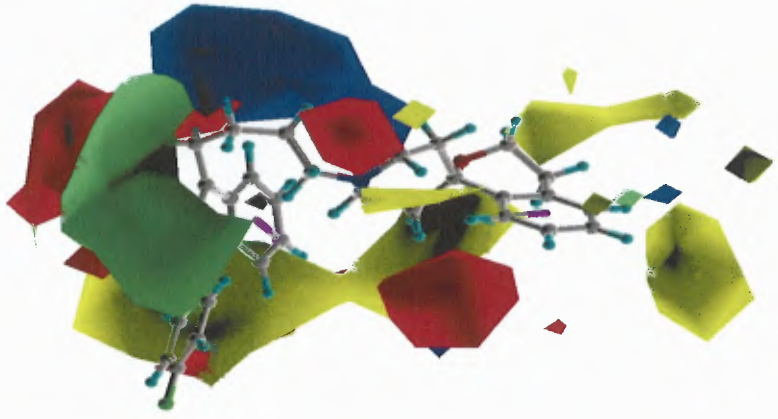

(b)

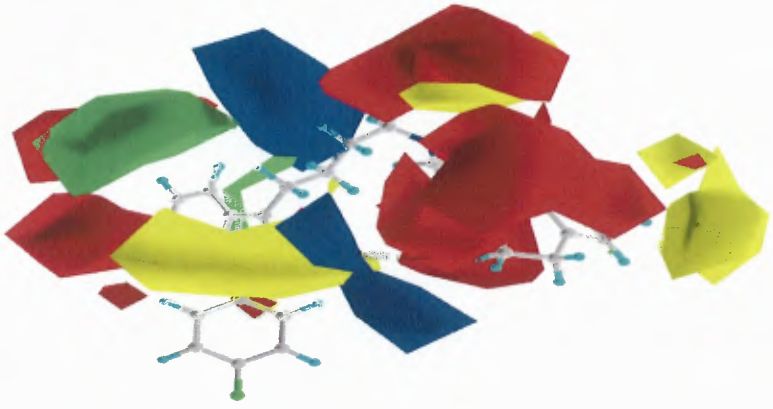

(c)

Figure 3.3 CoMFA contour maps derived by σ_2 receptor ligands using various charge and geometry optimization; AM1 (a), HF/6-31G* (b) and B3LYP/6-31G* (c) methods for Compound 26.

CHAPTER 4

RESULTS AND DISCUSSION

4.1 Pharmacophore

The pharmacophore designed by DISCOtech for σ_2 receptor ligands is a three point arrangement Figure 2.1 that includes a nitrogen atom and two hydrophobic centers. The two active σ_2 ligands (6) and (26) are represented in Figure 2.1 (b) and 2.2 (c) with the pharmacophore dimensions.

4.2 Comparative Molecular Field Analysis

The higher r^2 and F-value indicate higher accuracy. The non-crossvalidated PLS analysis produced the best r^2 and standard errors of predicted pK_i value. The obtained value of r^2, standard error of estimate and F value for all 22 compounds of training set using three calculation methods is reported in Table 3.4. The relationship between calculated and predicted pK_i values of training set of 22 compounds and a test set of 4 compounds by all three calculation methods using non-cross validated analysis is also reported in Table 3.2 and Table 3.3 respectively. The Graph of the predicted pK_i versus the actual pK_i values are shown in Figure 3.2. The CoMFA model was also cross-validated to confirm the predictive power of the model. The CoMFA model required three or four optimal components in different calculations to explain the variance in binding affinity to σ_2 receptors for this study. A q^2 value of more than 0.4 was obtained for all cross validated analyses. A $q^2 = 0.602$ at 4 component was obtained for B3LYP/6-31G* optimized geometries and atomic charge calculations; which was higher than those obtained with

AM1 and HF/6-31G* optimized geometries. The CoMFA models of AM1 optimized geometries produced lower q^2 of 0.417 than those of HF/6-31G* and B3LYP/6-31G* optimized geometries. The numerical results of a cross validated PLS analysis by "Leave-One-Out" method using the 22 compounds by all three calculation method are listed in Table 3.1.

4.3 Validation of the CoMFA Model

The four test compounds were selected; those include: 2 (Table 1.2), 5 (Table 1.3), 11 (Table 1.4) and 19 (Table 1.5); one from each major class of compounds. The range of binding affinities for the training set was -2.455 to 0.469 log units and the predicted range of pK_i for training set was -2.537 to 0.476 log units for AM1/6-31G* method, -2.454 to 0.454 log units for HF/6-31G* and -2.469 to 0.466 log units for B3LYP/6-31G* method Table 3.2. The bio-activity of all 22 ligands in the training set was predicted satisfactorily by all three calculation methods. The predictive utilities of CoMFA model for four ligands in the test set were considered satisfactory for all three calculations Table 3.3.

4.4 Design of New Ligands

The design of new ligands and prediction of activities is possible by using the spatial distribution of steric and electrostatic properties of CoMFA contour maps and its calculation (Figure 3.3). The Spiro [(2) benzopyran-1, 4'-piperidine] derivative (26) was one of the most potent and highly selective σ_2 receptor ligands. Six new structures were suggested in Table 4.1, and predicted pK_i values were calculated using AM1, HF/6-31G*, and B3LYP/6-31G* calculations.

The AM1 model failed to predict Spiro derivative (26) in the proper ranges (Table 4.1). The HF/6-31G* and B3LYP/6-31G* model had the higher q^2 values than the AM1 model therefore the predicted bioactivities of the new ligands are more probable by these two models. The CoMFA contour maps were investigated to find out locations where the modifications of substituent groups are essential to determine the effect on σ_2 activity. The CoMFA contour maps of steric fields are shown in yellow and green. The steric regions define the size and shape of the substituents around the molecule. The green areas where more bulky substituents are favoured, and yellow where less bulk is desired for higher σ_2 activity. The contour maps of electrostatic fields are shown in red and blue colors. The red regions favor more negative charge, and blue areas favor more positive charge for higher σ_2 activity. By using the knowledge of spatial distribution of steric and electrostatic regions, two locations on the CoMFA maps were investigated to determine the activity of designed new compounds (Table 4.1). These two important modification sites were represented by R_1 and R_2 on Spiro [(2) benzopyran-1, 4'-piperidine] derivative (26). Six new structures were constructed by changing substituent groups on R_1 and R_2. Among these new structures, compounds 27 and 28 had more bulky substituent groups at R_1 while compounds 29 and 30 had less bulky substituent groups at R_1 compared to the original ligand (26). By increasing bulk at R_1, a drop in the predicted pK_i value for compounds 27 (predicted pK_i=0.216) and 28 (predicted pK_i=0.211) was observed from the original ligand 26, using the HF/6-31G* PLS analysis while an increase predicted pK_i value for these two compounds (Table 4.1) was observed using B3LYP/6-31G* PLS analysis. Compounds 29 and 30 have less bulky substituents at R_1, which shows higher predicted σ_2 activity for HF/6-31G* and also for B3LYP/6-31G* PLS analysis.

The predicted pK_i value for compounds 29 and 30 are -0.498 and -0.519 for HF/6-31G* analysis, while -0.651 and -0.022 for B3LYP/6-31G* analysis respectively. The R_1 position of substituent groups falls in the yellow areas where less steric bulk is favored for higher σ_2 activity so the values of compounds 29 and 30 clearly suggest that less bulk at R_1 is favorable for higher σ_2 activity.

The R_2 position of substituent groups falls in the red areas where more negative charge is favored for higher σ_2 activity. Compounds 31 and 32 contain negative charged substituent groups at R_2. By introducing a methoxy ($-OCH_3$) group at R_2 position in compound 32 an increase in predicted σ_2 activity (0.043) for HF/6-31G* and (-0.292) for B3LYP/6-31G* PLS analysis compared to the bioactivity of the original ligand 26 (Table 4.1). This study suggests that, there is a possibility for future development of σ_2 receptor ligands by using small substituent groups at R_1 and by using electronegative substituent groups at R_2 to increase selectivity and affinity of these ligands.

Table 4.1 Prediction of Bioactivity for New Ligands

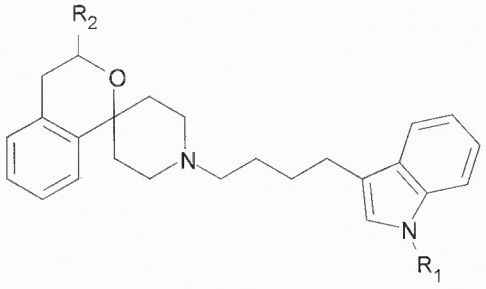

Compounds	Lit. (pK_i)	R_1	R_2	AM1	HF/6-31G*	B3LYP/6-31G*
				Predicted pK_i		
26	0.155	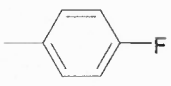	-H	0.229	0.159	0.112
27	-	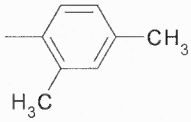	-H	-0.209	0.216	-0.261
28	-	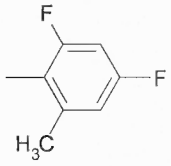	-H	-0.313	0.211	-0.036
29	-	$-CH_3$	-H	0.211	-0.498	-0.651
30	-	-H	-H	0.110	-0.519	-0.022
31	-		-OH	-0.211	0.154	0.219
32	-	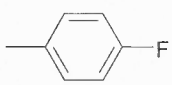	$-OCH_3$	0.125	0.043	-0.292

CHAPTER 5

CONCLUSIONS

This study derived a pharmacophore model that should aid in the design of additional ligands which possess high affinity and selectivity for the σ_2 receptor. The predicting power of the CoMFA models was tested and verified using PLS cross validation. Three CoMFA contour map were obtained with an alignment of 26 compounds whose geometries and atomic charge were optimized in AM1, HF/6-31G*, and B3LYP/6-31G*. This study also suggested that B3LYP/6-31G* optimized geometries produced good CoMFA models to predict bioactivity of σ_2 ligands. Two possible sites of modification for most potent and highly selective σ_2 ligand (26) were represented by R_1 and R_2. Addition of less bulky groups at R_1 and more electronegative groups at R_2 produced more active σ_2 receptor ligands.

REFERENCES

[1] W. R. Martin, C. G. Eades, J. A. Thompson, R. E. Huppler, and P. E. J. Gilbert, *Pharmacol. Exp. Ther.,* vol. 197, pp. 517-532, 1976.

[2] J. M. Walker, W. D. Bowen, F. O. Walker, R. R. Matsumoto, B. d. Costa, and K. Rice, *C. Pharmacol. Rev.,* vol. 42, pp. 355-402 1990.

[3] M. W. Scherz, M. Fialeix, J. B. Fischer, L. N. Reddy, A. C. Server, M. S. Sonders, B. C. Tester, E. Weber, S. T. Wong, and J. F. W. Keana, *J. Med. Chem.,* vol. 33, pp. 2421-2429 1990.

[4] C. Kaiser, J. Pontecorvo, and R. E. Mewshaw, *Neurotransmission,* vol. 7, pp. 1-5, 1991.

[5] W. D. Bowen, *Pharm. Acta Helv.,* vol. 74, pp. 211-218, 2000.

[6] R. Quirion, W. D. Bowen, Y. Itzhak, J. L. Junien, J. M. Musacchio, R. B. Rothman, T. P. Su, S. W. Tam, and D. P. Taylor, *Trends Pharmacol. Sci.,* vol. 13, pp. 85-86, 1992.

[7] S. D. Wyrick and R. G. Booth, *Drugs Future,* vol. 20, pp. 1033-1044, 1995.

[8] M. Hanner, F. F. Moebius, A. Flandorfer, and H. G. Knaus, *Proc. Natl. Acad. Sci. U.S.A.,* vol. 93, pp. 8072-8077, 1996.

[9] R. Kekuda, P. D. Prasad, Y. J. Fei, F. H. Leibach, and V. Ganapathy, *Biochem. Biophys. Res. Commun.,* vol. 229, pp. 553-558, 1996.

[10] P. Seth, Y. J. Fei, H. W. Li, W. Huang, F. H. Leibach, and V. J. Ganapathy, *J. Neurochem.,* vol. 70, pp. 922-932, 1998.

[11] S. B. Hellewell, A. Bruce, G. Feinstein, J. Orringer, W. Williams, and W. D. Bowen, *Eur. J. Pharmacol.,* vol. 268, pp. 9-18, 1994.

[12] A. M. Myers, P. S. Charifson, C. E. Owens, N. S. Kula, A. T. McPhail, R. J. Baldessarini, R. G. Booth, and S. D. Wyrick, *J. Med. Chem.,* vol. 37, pp. 4109-4117 1994.

[13] Z. Lin and P. K. Kabada, *Med. Res. Rev.,* vol. 17, pp. 537-572, 1997.

[14] H. Ujike, S. Kuroda, and S. Otsuki, *Eur. J. Pharmacol.,* vol. 296, pp. 123-128, 1996.

[15] C. S. John, B. B. Lim, B. J. Vilner, B. C. Geyer, and W. D. Bowen, *J. Med. Chem.,* vol. 41, pp. 2445-2450, 1998.

[16] T. Maurice and B. P. Lockhart, *Prog. Neuro-Psycho-Pharmacol. Biol. Psychiatry,* vol. 21, pp. 69-102, 1997.

[17] T. L. Collier, R. N. Waterhouse, and M. Kassiou, *Current Pharmaceutical Design,* vol. 13, pp. 51-72, 2007.

[18] J. C. Jaen, B. W. Caprathe, T. A. Pugsley, L. D. Wise, and H. Akunne, *J. Med. Chem.,* vol. 36, pp. 3929-3936, 1993.

[19] S. M. N. Efange, R. H. Mach, C. R. Smith, A. B. Khare, C. Foulon, S. K. Akella, S. R. Childer, and S. M. Parsons, *Biochem. Pharmacol.,* vol. 49, p. 791, 1995.

[20] V. H. Nguyen, M. Kassiou, G. A. R. Johnston, and M. J. Christie, *Eur. J. Pharmacol.,* vol. 311, pp. 233-240, 1996.

[21] W. D. Bowen, C. M. Bertha, B. J. Vilner, and K. C. Rice, *Eur. J. Pharmacol.,* vol. 278, pp. 257-260, 1995.

[22] A. Yamashita, N. Takahashi, D. Mochizuki, R. Tsujita, S. Yamada, H. Kawakubo, Y. Suzuki, and H. Watanabe, *Bioorg. Med. Chem. Lett.,* vol. 7, pp. 2303-2306, 1997.

[23] F. Berardi, S. Ferorelli, C. Abate, N. A. Colabufo, M. Contino, R. Perrone, and V. Tortorella, *J. Med. Chem.,* vol. 47, pp. 2308-2317, 2004.

[24] L. Costantino, F. Gandolfi, C. Sorbi, S. Franchini, O. Prezzavento, F. Vittorio, G. Ronsisvalle, A. Leonardi, E. Poggesi, and L. Brasili, *J. Med. Chem.,* vol. 48, pp. 266-273, 2006.

[25] S. Vangveravong, J. Xu, C. Zeng, and R. H. Mach, *Bioorg. Med. Chem.,* vol. 14, pp. 6988-6997, 2006.

[26] D. T. Manallack, M. G. Wong, M. Costa, P. R. Andrews, and P. M. Beart, *Mol. Pharm.,* vol. 34, pp. 863-879, 1988.

[27] R. A. Glennon, S. Y. Ablordeppey, A. M. Ismaiel, M. B. El-Ashmawy, and J. B. Fischer, *J. Med. Chem.,* vol. 37, pp. 1214-1219, 1994.

[28] T. M. Gund, J. Floyd, and D. Jung, *J. Mol. Graph. Modell.,* vol. 22, pp. 221-230, 2004.

[29] C. Laggner, C. Schieferer, B. Fiechtner, G. Poles, R. D. Hoffmann, H. Glossmann, T. Langer, and F. F. Moebius, *J. Med. Chem.*, vol. 48, pp. 4754-4764, 2005.

[30] P. Cratteri, M. N. Romanelli, G. Cruciani, C. Bonaccini, and F. Melani, *J. Comp. Aided. Mol. Des.*, vol. 18, pp. 361-374, 2004.

[31] SYBYL 7.3, Tripos Associates, Inc.: St. Louis, MO, 2006.

[32] M. J. Frisch, G. W. Trucks, H. B. Schlegel, G. E. Scuseria, M. A. Robb, J. R. Cheeseman, V. G. Zakrzewski, J. A. Montgomery, J. R. E. Stratmann, J. C. Burant, S. Dapprich, J. M. Millam, A. D. Daniels, K. N. Kudin, M. C. Strain, O. Farkas, J. Tomasi, V. Barone, M. Cossi, R. Cammi, B. Mennucci, C. Pomelli, C. Adamo, S. Clifford, J. Ochteski, G. A. Petersson, P. Y. Ayala, Q. Cui, K. Morokuma, P. Salavador, J. J. Dannenberg, D. K. Malick, A. D. Rabuck, K. Raghavachari, J. B. Foresman, J. Cioslowski, J. V. Ortiz, A. G. Baboul, B. B. Stefanov, G. Liu, A. Liashenko, P. Piskorz, I. Komaromi, R. Gomperts, R. L. Martin, D. J. Fox, T. Keith, M. A. Al-Laham, C. Y. Peng, A. Nanayakkara, M. Challacombe, P. M. W. Gill, B. Johnson, W. Chen, M. W. Wong, J. L. Andres, C. Gonzalez, M. Head-Gordon, E. S. Replogle, and J. A. Pople, Gaussian 98, Gaussian, Inc. Pittsburgh PA, 2001.

[33] H. Gohlke and G. Klebe, "Approaches to the description and prediction of the binding affinity of small-molecule ligands to macromolecular receptors," *Angewandte Chemie International Edition,* vol. 41, pp. 2644-2676, 2002.

[34] J. S. Mason, A. C. Good, and E. J. Martin, "3-D pharmacophores in drug discovery," *Current Pharmaceutical Design,* vol. 7, pp. 567-597, 2001.

[35] Y. C. Martin, M. G. Bures, E. A. Dahaner, J. Delazzer, I. Lico, and P. A. Pavlik, *J. Comp. Aided. Mol. Des.*, vol. 7, pp. 83-102, 1993.

[36] C. Sköld and A. Karlén, "Development of CoMFA models of affinity and selectivity to angiotensin II type-1 and type-2 receptors," *Journal of Molecular Graphics and Modelling,* vol. 26, pp. 145-153, 2007.

[37] T. M. Gund, D. Jung, and J. Floyd, *J. Comp. Chem.*, vol. 25, pp. 1385-1399, 2003.

[38] O. Guner, O. Clement, and Y. Kurogi, *Curr. Med. Chem.*, vol. 11, pp. 2991-3005, 2004.

[39] D. Zampieri, M. G. Mamolo, E. Laurini, C. Florio, C. Zanette, M. Fermeglia, P. Posocco, M. S. Paneni, S. Pricl, and L. Vio, *J. Med. Chem.*, vol. 52, pp. 5380-5393, 2009.

[40] R. D. Cramer, D. E. Patterson, and J. D. Bunce, *J. Am. Chem. Soc.,* vol. 110, pp. 5959-5967, 1998.

[41] B. L. Bush and R. B. Nachbar, *J. Comp. Aided. Mol. Des.,* vol. 7, pp. 587-619, 1993.

[42] S. Wold, E. Johansson, and M. Cocchi, "3D QSAR in Drug Design. Theory, Methods and Applications," *PLS-Partial Least Squares Projection to Latent Structures. ESCOM, Lieden,* pp. 523–550, 1993.

[43] R. D. Cramer, J. D. Bunce, D. Patterson, and I. E. Frank, *Quant. Struct.-Act. Relat.,* vol. 7, pp. 18-25, 1998.

[44] J. M. Rieger, M. L. Brown, G. W. Sullivan, J. Linden, and T. L. Macdonald, *J. Med. Chem.,* vol. 44, pp. 531-539, 2001.